IEEE Access
Multidisciplinary ⋮ Rapid Review ⋮ Open Access Journal

Received 5 November 2023, accepted 22 November 2023, date of publication 4 December 2023,
date of current version 18 December 2023.

Digital Object Identifier 10.1109/ACCESS.2023.3339377

APPLIED RESEARCH

Test and Analysis on Electromagnetic Disturbance of Digital Unit of Primary–Secondary Integrated 10kV Circuit Breaker

FEIYAN ZHOU[1], YAN WU[1], LINGYUN GU[1], DINGYU QIN[2], CHONGQING JIAO[2], ZHANPENG DU[2], ZUOXING DENG[2], ZHIYE JIANG[2], AND JIANCHENG HUANG[2]

[1]China Electric Power Research Institute, Beijing 100192, China
[2]State Key Laboratory of Alternate Electrical Power System with Renewable Energy Source, North China Electric Power University, Beijing 102206, China

Corresponding author: Chongqing Jiao (cqjiao@ncepu.edu.cn)

This work was supported by the Study on Failure Mechanism and Protection Technology of Measurement Transfer for Primary and Secondary Fused Distribution Equipment under Grant 5400-202355734A-3-3-JC.

ABSTRACT The primary side and secondary side of the 10-kV digital circuit breaker is deeply integrated. Wherein, an electronic transformer is deployed together with the breaker inside a cabinet, and a digital unit is closely connected to the output port of the electronic transform. This compact and close arrangement makes the secondary side face a severe electromagnetic environment during the switching operation of the breaker. In this paper, we report the measured electromagnetic disturbances resulting from the opening/closing of 20 kA current by the breaker. The results show that the disturbance voltage at the secondary side port of the voltage transformer has the waveform of damped oscillatory waves, a peak value of up to 1.1kV, and dominant frequencies of 4.4 MHz and 15 MHz. The disturbance voltage at the secondary side port of the current transformer has a peak value of 350 V. The peak value of dH/dt of the spatial magnetic field is 0.387 kA·m^{-1} · μs^{-1}. By comparing the measured waveforms with these specified in IEC 61000-4-18 and IEC 61000-4-10 standards, we advise that the level of immunity test is the third level of the fast-damped oscillatory wave for voltage port and the fourth level of the damped oscillatory magnetic for enclosure port.

INDEX TERMS Electromagnetic disturbance, electromagnetic compatibility (EMC), primary and secondary integrated, switching operation, short-circuit current breaking, damped oscillatory wave.

I. INTRODUCTION

With the continuous development of digital transformation of the distribution network, the new 10 kV distribution switch adopts advanced assembly processes such as primary and secondary deep integration to achieve the ''miniaturization, integration, and interchangeability'' of the whole equipment. The primary and secondary integration standardized column circuit breaker equipped with electronic transformers and digital units has been included in the bidding and construction tasks of the distribution network protocol inventory of the State Grid Corporation of China and is gradually replacing the traditional medium voltage complete equipment. However, its design scheme of deep integration of multiple sensing units and digital units puts forward higher requirements for the EMC of the equipment body. It is necessary to further evaluate the anti-electromagnetic interference capability of the new medium voltage distribution network digital equipment under the high-intensity electromagnetic interference environment such as surge impact, short circuit making, breaking, high-power capacitive load switching, etc. When the distribution switch switches on and off the short-circuit current, the strong electromagnetic interference conduction coupling mechanism between the primary and secondary strong and weak current components inside the equipment is more complex and harsher. The failure of distribution line fault handling, protection failure or maloperation, and other safety problems caused by the performance degradation or

The associate editor coordinating the review of this manuscript and approving it for publication was Mehmet Alper Uslu.

failure of core secondary components have become one of the prominent hidden dangers that directly affect the safety and operation safety of distribution network equipment.

There are essential differences between electronic sensors and traditional electromagnetic transformers in principle and transmission characteristics. The output signal strength of the secondary side of the electronic transformer is much lower than that of the electromagnetic transformer, and the distance between the secondary equipment and the primary system can be as close as 0.3 m, which makes the electromagnetic disturbance more prominent. However, the current EMC immunity assessment standards and test methods for distribution switch secondary equipment are based on the summary of electromagnetic transformer test experience and cannot be directly applied to electronic sensors. In recent years, for the secondary equipment near the high-voltage switch in the substation, the immunity standard of the damped oscillatory wave has been updated, and the rapid damped oscillatory wave assessment items of 3 MHz, 10 MHz, and 30 MHz have been added [1], [2], [3]. However, the research on application scenarios of distribution switches is less. To adjust the EMC immunity assessment standard of secondary equipment adaptively, it is necessary to master its electromagnetic disturbance characteristics. Due to the wide range of electromagnetic disturbance frequency bands, the modeling and simulation of the switch require a detailed understanding of the internal structure of the switch and the transmission characteristics of the transformer. Unfortunately, the conditions are often not available, and the site conditions are complex, so it is difficult to obtain the specific parameters of the switch, resulting in great difficulty in modeling. Therefore, field experiments are usually used to obtain electromagnetic disturbance characteristics.

For switch electromagnetic disturbance, the existing research mainly focuses on the electromagnetic transient problem caused by the operation of substation disconnectors. On this basis, the EMC immunity assessment criteria for secondary equipment such as substation control and protection are further proposed, while the existing research on distribution switch application scenarios is less [4], [5], [6], [7], [8], [9], [10], [11], [12], [13], [14], [15], [16], [17], [18], [19], [20], [21], [22], [23], [24], [25], [26], [27]. For the distribution network switch cabinet, Li Yuling and others tested the disturbance voltage waveform at the secondary side of the electronic transformer at the moment of opening and closing of the circuit breaker during no-load and capacitive load switching. The peak value is about 110 V, and the main frequency is between 1∼30 MHz. However, the high current short-circuit on-off condition is not involved, and the number of tests is small [28]. For a 10-kV pole-mounted switch, Li Peng et al. conducted a single-phase breaking test by using an oscillating synthetic test circuit. The results showed that the secondary side interference of the current transformer caused by the switch breaking and arcing process was mainly distributed in the frequency band 7.81∼15.62 MHz, but the disturbance amplitude was not studied in depth [29]. Niu Bo et al. conducted a capacitive closing test on a 10kV switch by using a synthetic circuit and obtained that when the closing current amplitude is 20kA and the frequency is 4.25 kHz, the electric field interference amplitude can reach 12.56 kV/m, the magnetic field interference amplitude can reach 26.23 A/m, and the main frequency can reach hundreds of MHz's However, the closing current is not considered as power frequency [30]. Many measured results show that the secondary side of the primary and secondary integrated column circuit breaker transformer will produce a high-frequency damped oscillatory wave with high amplitude now of switching operation [31].

In addition, domestic scholars have also carried out some research on the electromagnetic disturbance on the secondary side of the primary and secondary integration column circuit breaker (PSICCB) transformer under lightning-stroke conditions. The results show that although the lightning wave with a dominant frequency lower than 1 MHz is applied to the primary side, the damped oscillatory wave with a frequency up to tens of MHz can also be caused at the secondary side, which will greatly affect the accuracy of the AD acquisition module in the FTU [32], [33], [34]. It should be noted that, due to the complex configuration of the breakers and the randomness of arcing during switching operation, the numerical simulation is usually too difficult to implement. Hence, in-site testing is usually the main technical approach to obtaining electromagnetic disturbance waveforms.

At present, the research on electromagnetic disturbance of primary and secondary integrated column circuit breakers under the condition of short circuit making and breaking large current is very limited, and the influence of electromagnetic disturbance may be more serious. In this paper, through the electromagnetic disturbance experiment of 20 kA power frequency current for short circuit making and breaking of the PSICCB, the disturbance voltages of the secondary side phase voltage port, line current port, zero-sequence voltage port, and zero-sequence current port of the transformer now of switch opening and closing are obtained. In addition, the induced voltage of the space magnetic field near the incoming line side and the voltage of the switch enclosure to the ground are also measured. Based on the measured results, we put forward some suggestions on the immunity of the primary and secondary integrated column circuit breakers to the secondary side of the transformer and the assessment standard of the space magnetic field under the condition of short circuit making and breaking large current. However, the relation between the severity of the electromagnetic disturbances and the reliability of the system is not investigated in this article. To do that, the intensity of electromagnetic disturbance needs to be increased continuously and meanwhile one should observe when the equipment under test will exhibit abnormal behavior.

Considering safety and necessity, manufacturers or users generally do not intend to provide testing opportunities, especially for multiple high current breaking cases. Therefore, such test results appear to be very valuable.

II. MEASURING SYSTEM AND PLATFORM

A. MEASURING SYSTEM

The transient measurement system used in this experiment is mainly composed of the voltage divider, oscilloscope (Tektronix DMO3104), optical fiber control system, inverter, lithium battery, and shielding box, and its principle is the same as that of the electromagnetic disturbance experiment measurement system for switching operation of substation [3], [35], [36], [37]. The transient measurement system has good EMC through a battery power supply, photoelectric conversion, external shielding box, and other methods. The range of voltage divider selected during measurement can reach 7 kV, and the bandwidth is 120 MHz; The bandwidth of the oscilloscope used can reach 1 GHz, and the maximum sampling rate is 5 GSa/s. A metallic box is used to enclose the oscilloscope to provide electromagnetic shielding. Such boxes had been employed in our previous tests [1], [2], [3], [35], [36].

B. MEASURING PLATFORM

Figure 1 is the PSICCB under test (ZW32E-12/T630-20), and its main parameters are shown in Table 1. The 20-kA high current switching test of the circuit breaker was carried out using the large capacity group monitoring platform of Changzhou Co., Ltd. of Xi'an High Voltage Apparatus Research Institute. It is powered by a three-phase power supply, with a power supply voltage of 12 kV, and the load side is always short-circuited. This experiment measured the disturbance voltage on the phase voltage port, current port, zero-sequence voltage port, and zero-sequence current port of the secondary side of the transformer when the circuit breaker opened and closed 20 kA current and when the circuit breaker opened 20 kA current. The measuring equipment uses high-voltage probes (Pintech P6039A and Pintech P6010A) and a home-made toroidal coil with electric shielding (The 5-turn loop with a diameter of 15cm). The acquisition device uses an oscilloscope. The measuring equipment uses high-pressure probes (Pintech P6039A and Pintech P6010A) and, a home-made toroidal coil with electric shielding (The 5-turn loop with a diameter of 15 cm). The acquisition device uses an oscilloscope.

The circuit principle of the electronic transformer and the schematic diagram of the tested signal port terminals are shown in Fig. 2, and the tested signal ports and corresponding terminals are shown in Table 2. The flow chart of the test process is shown in Fig.3. In addition, this test also measured the space magnetic field-induced voltage and the voltage of the switch enclosure to the ground. The induced voltage of the space magnetic field is measured by a 5-turn loop with a diameter of 15 cm, which is placed 1m below the incoming line side of the switch. When measuring the enclosure-to-ground voltage, the terminal blocks are connected to the enclosure measuring points as shown in Fig. 1, and the grounding busbar at 2 m from the switch. Since the potential sensitive equipment/devices are usually installed on the secondary side, only the electromagnetic disturbances on the secondary side are measured. In practice, transient voltage surges can also occur on the primary side and need to be measured, especially when such transients may cause electrical insulation problems.

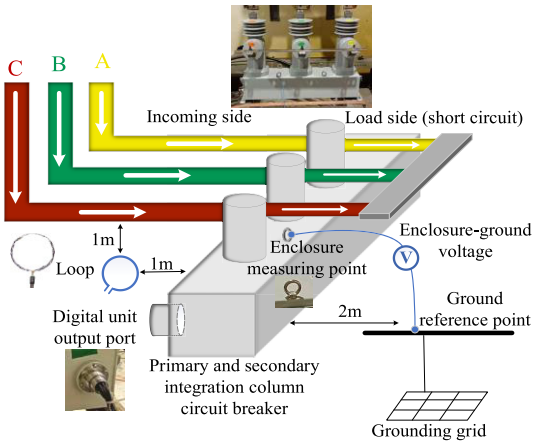

FIGURE 1. Primary and secondary integration column circuit breaker.

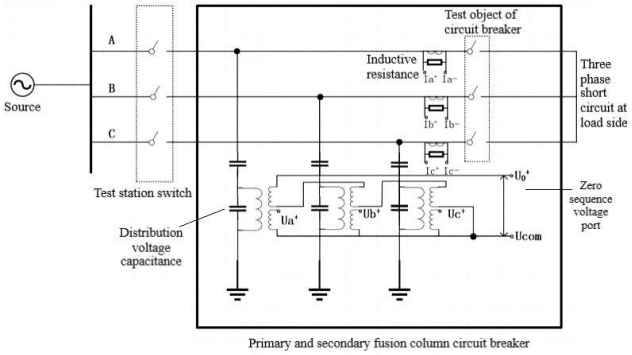

FIGURE 2. Schematic of circuit principle of electronic transformer.

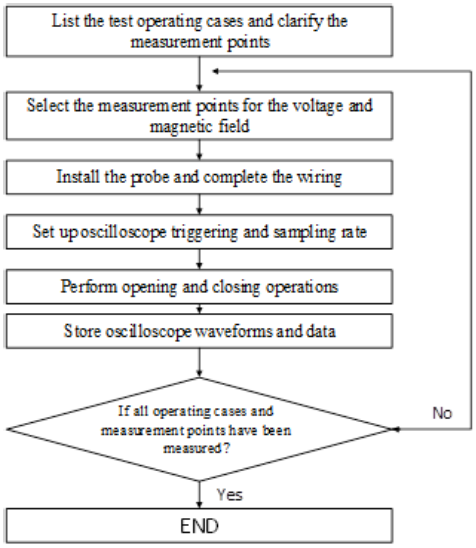

FIGURE 3. Test flow chart of the test process for the transient electromagnetic disturbances.

TABLE 1. Technical parameters of circuit breaker.

Category	Unit	Technical requirements
Rated voltage	kV	12
Rated Current	A	630
Rated frequency	Hz	50
Rated breaking short-circuit current	kA	20
Rated thermal stability current (effective value)	kA	20
Rated thermal stability time	s	4
Rated short-circuit-making current (peak)	kA	50
Rated dynamic stability current (peak)	kA	50
Lightning impulse test voltage	kV/min	75/85
Rated current ratio		600A/1V
Zero-sequence current		20A/0.2V
Phase voltage		(10kV/√3)/(3.25V/√3)
Zero-sequence voltage		(10kV/√3)/(6.5V/√3)

TABLE 2. The corresponding terminal of the measured signal port.

Signal port	Measuring terminal positive	Measuring terminal cathode [a]
A-phase voltage port	Ua+	Ucom
C-phase voltage port	Uc+	Ucom
Zero sequence voltage port	U0+	Ucom
A-phase current port	Ia+	Ia-
C-phase current port	Ic+	Ic-
Zero-sequence current port	I0+	I0-

III. MEASUREMENT OF DISTURBANCE VOLTAGE GENERATED BY SHORT CIRCUIT MAKING AND BREAKING

A. CLOSING AND OPENING OF CIRCUIT BREAKER 20kA CURRENT

In the case of a short circuit on the load side, the initial state of the circuit breaker is the breaking state. The 20 kA current is switched on first and then switched off. The test has been carried out 3 times in total, and the results have good repeatability. The action sequence is that the test station switch is closed, the circuit breaker is closed after 67.7 ms, the circuit breaker is opened after 52.8 ms, and finally, the test station switch is opened after 84 ms. The whole process lasts about 200 ms. The electrical quantity waveform at the inlet side is shown in Fig. 4, with a phase voltage amplitude of 12 kV and a current amplitude of 20 kA.

1) PHASE A VOLTAGE PORT AT THE SECONDARY SIDE OF THE TRANSFORMER

The voltage waveform of the phase A voltage port on the secondary side of the transformer under the condition of 20 kA current closing and opening of the circuit breaker is shown in Fig. 5. When the circuit breaker is closed (t=0.00 s) and opened (about t=0.053 s), there are pulses with large amplitude. The waveform time of the two pulse signals is expanded as shown in Fig. 6 and Fig. 7. In Fig. 6(a), two damped oscillatory signals appear at the A-phase voltage

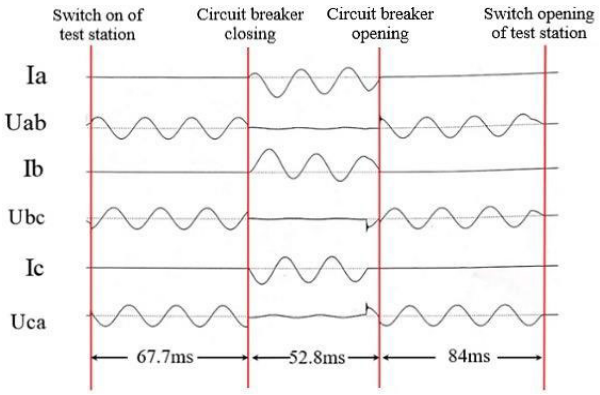

FIGURE 4. Electric quantity waveform diagram of the primary side under closing-opening conditions.

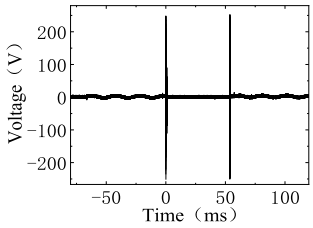

FIGURE 5. Macro pulse waveform of phase A voltage port when the circuit breaker is closing-opening.

port on the secondary side of the transformer now of circuit breaker closing, and the total duration of the pulse is about 51.5 μs. The duration of the first damped oscillatory wave is about 16.46 μs, and the peak value is about 230 V; The second damped oscillatory wave has a duration of about 7.14 μs and a peak value of about 250 V. In Fig. 7(a), six damped oscillatory signals appear at the A-phase voltage port on the secondary side of the transformer at the moment of circuit breaker opening, with a total duration of about 185.66 μs, peak values of about 250 V, the average duration of 45 μs and basically the same interval between adjacent signals. The waveforms of the first section (t<0.00 s) and the third section (t>0.05 s) separated by the opening and closing instant in Fig.5 are power frequency signals under the normal conduction of the switch. The measured voltage amplitude at the secondary side and the primary side of the transformer meet the transformation ratio of the transformer.

The frequency domain analysis of the first damped oscillatory wave at the A-phase voltage port at the closing and opening moment of the circuit breaker is carried out respectively. The spectral density is shown in Fig. 8. The main frequency of the disturbance voltage at the closing moment is 4.43 MHz and 14.76 MHz, and the opening moment is 4.11 MHz.

2) PHASE C VOLTAGE PORT AT THE SECONDARY SIDE OF THE TRANSFORMER

The waveform of the C-phase voltage port at the secondary side of the transformer now of circuit breaker opening and closing is basically the same as that of the A-phase voltage

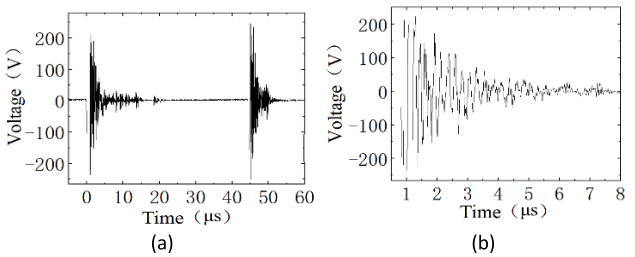

FIGURE 6. Micropulse waveform of phase A voltage port (Closing-opening operation: closing): (a) Complete pulse; (b) first damped oscillatory signal expansion.

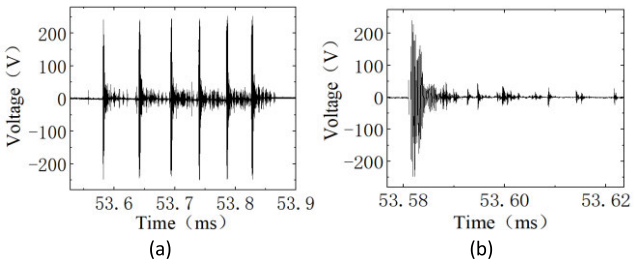

FIGURE 7. Micropulse waveform of phase A voltage port (Closing-opening operation: opening): (a)complete pulse; (b) first damped oscillatory signal expansion.

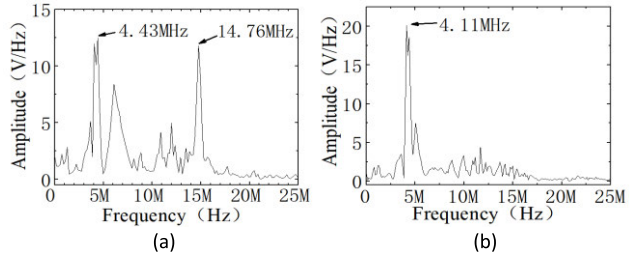

FIGURE 8. Disturbance voltage spectrum of phase A voltage port during circuit breaker opening and closing: (a) Closing-opening operation: closing (b) Closing-opening operation: opening.

port. The duration of the circuit breaker closing pulse signal is about 53.95 μs, which is also composed of two damped oscillatory signals. The duration of the first damped oscillatory wave is about 16.8μs, and the peak value is about 216 V; The second damped oscillatory wave has a duration of about 9.6 μs, a peak value of about 217 V, and a dominant frequency of 4.43 MHz, 6.11 MHz, and 18.33 MHz. At the moment of opening, six damped oscillatory signals also appear at the C-phase voltage port on the secondary side of the transformer. The total duration of the pulse is about 280.1 μs, the peak value is 220 V, and the average duration is 45 μs. The interval between adjacent signals is the same, and the dominant frequency is 4.41 MHz. Fig.9 shows one of the micro-pulses measured at the phase C voltage port at the moment of the closing for the closing-opening operation. Fig.10 displays one of the micro-pulses measured at the phase C voltage port at the moment of the opening for the closing-opening operation. The corresponding spectrums are plotted in Fig.10(a) and Fig.10(b), respectively.

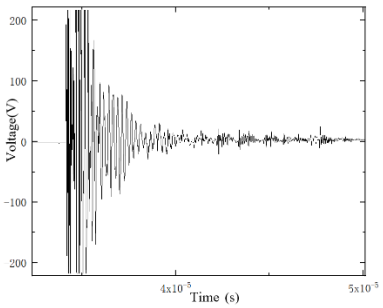

FIGURE 9. Micropulse waveform of phase C voltage port (Closing-opening operation: closing): first damped oscillatory signal expansion.

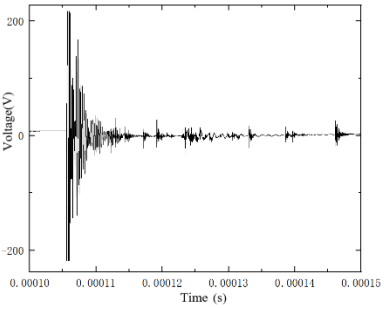

FIGURE 10. Micropulse waveform of phase C voltage port (Closing-opening operation: opening): first damped oscillatory signal expansion.

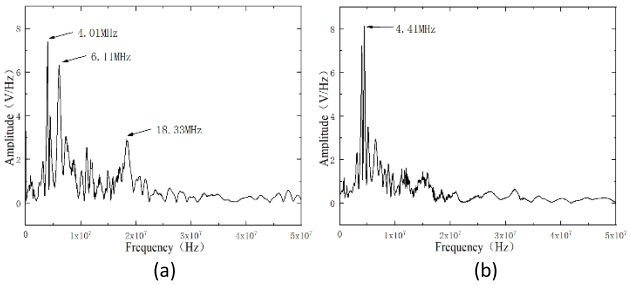

FIGURE 11. Disturbance voltage spectrum of phase C voltage port during circuit breaker opening and closing: (a) Closing-opening operation: closing (b) Closing-opening operation: opening.

3) ZERO-SEQUENCE VOLTAGE PORT AT THE SECONDARY SIDE OF THE TRANSFORMER

The time domain waveform of the zero-sequence voltage port at the moment of closing and opening of the circuit breaker is shown in Fig. 12. Pulse signals appear at the moment of closing and opening, with a peak value of 250 V. The pulse signal duration at the moment of closing is 51.5 μs, and the pulse duration at the moment of the opening is 286 μs. The micropulse waveform is shown in Fig. 13. The pulse signal of closing the circuit breaker is composed of two micro pulses with a peak value of 250 V and a duration of about 2 μs for each micropulse; The instantaneous opening pulse signal consists of 6 micro pulses, with a peak value of 250 V and an average duration of 3.5 μs.

4) PHASE A CURRENT PORT AT THE SECONDARY SIDE OF THE TRANSFORMER

When the circuit breaker is closing and opening, the disturbance voltage waveform of the phase A current port is shown

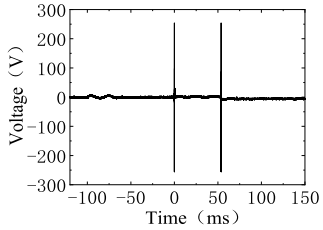

FIGURE 12. Time domain waveform of zero-sequence voltage port for closing and opening of the circuit breaker.

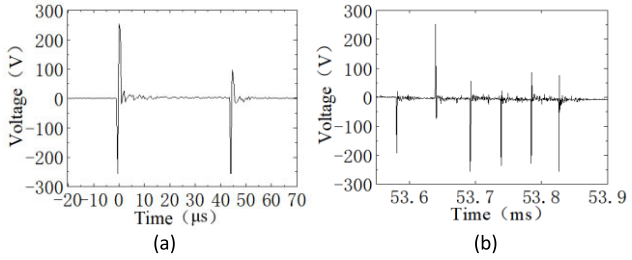

FIGURE 13. Micropulse waveform of zero-sequence voltage port when the circuit breaker is closing-opening: (a) closing: pulse signal expansion; (b) opening: pulse signal expansion.

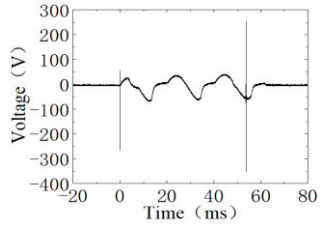

FIGURE 14. Time domain waveform of phase A voltage port for closing-opening of the circuit breaker.

in Fig. 14. Pulse signals appear at the moment of closing and opening, and the micropulse waveform is shown in Fig. 15. The total duration of the pulse at the closing moment of the circuit breaker is about 51 μs, consisting of two micro pulses, of which the first micro pulse peak value is 54 V, the second micro pulse peak value is 266 V, and the duration of each micropulse is about 3 μs; The total duration of the instantaneous opening pulse signal is about 272 μs, which is composed of 6 micro pulses. The minimum peak value is 75 V, the maximum value is 350 V, and the average duration is 3.5 μs.

The power frequency waveform between closing and opening time in Fig. 14 is not a perfect 50 Hz sine wave. Through waveform analysis, it is found that the positive and negative half-circumference areas are equal, so there is no DC component, but there should be a high-order harmonic component. The occurrence of the high-order harmonic component may be caused by the nonlinearity of the iron core under high currents. When the distribution switch operates normally with load, the current passing through the switch does not exceed a few kA, and the iron core in the current transformer may be saturated under a large current of 20 kA, resulting in harmonic generation and waveform distortion. It can be seen from the transformer's transformation ratio that the measured

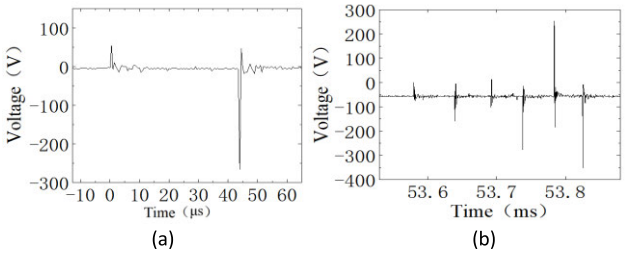

FIGURE 15. Micropulse waveform of phase A voltage port when the circuit breaker is closing-opening: (a) closing: pulse signal expansion; (b) opening: pulse signal expansion.

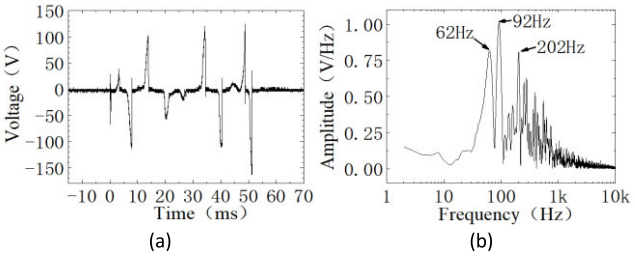

FIGURE 16. Zero-sequence current port voltage at the secondary side of the transformer when the circuit breaker is closing-opening: (a)time domain waveform; (b) amplitude-frequency characteristic.

waveform amplitude corresponds to the primary side voltage of 10 kV, which can prove that the measurement of the power frequency signal by the measurement system is accurate.

5) ZERO-SEQUENCE CURRENT PORT AT THE SECONDARY SIDE OF THE TRANSFORMER

The voltage waveform and spectrum of the zero-sequence current port of the circuit breaker closing, and opening are shown in Fig. 16. The duration is about 52 ms, and it is composed of 10 micro pulses. The minimum peak value of the micropulse is 40 V, the maximum value is 160 V, and the main frequency is 92 Hz, 62 Hz, and 202 Hz.

B. CIRCUIT BREAKER OPENING 20kA CURRENT

The load side is short-circuited, the initial state of the circuit breaker is closed, and the 20 kA current is cut off. The test has been carried out 8 times, with good repeatability. The action sequence takes the closing moment of the test station switch as the time starting point, the circuit breaker opens after 73.8 ms, and then the test station switch opens after 126 ms. The electrical quantity waveform at the inlet side is shown in Fig. 17.

1) PHASE C VOLTAGE PORT AT THE SECONDARY SIDE OF THE TRANSFORMER

When the circuit breaker opens 20 kA current, the disturbance voltage waveform and corresponding frequency spectrum of the phase C voltage port at the secondary side of the transformer are shown in Fig. 18(a) and Fig. 18(b) respectively. A damped oscillatory wave signal with a peak value of 1.1 kV appears at the moment of opening, with a duration of 6.04 μs and a dominant frequency of 4.43 MHz.

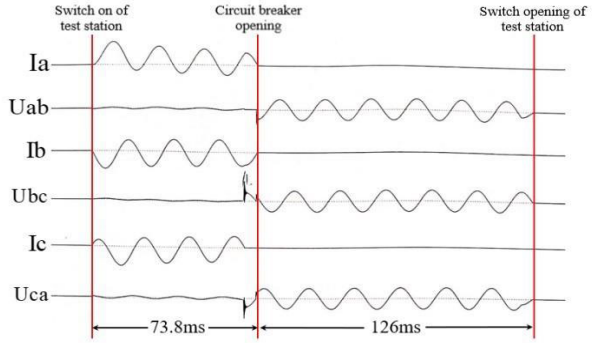

FIGURE 17. Electric quantity waveform at the primary side under opening conditions.

The IEC 61000-4-18 standard [39] especially relates to the immunity and test methods for damped oscillatory waves, which are usually generated by the switching operation of circuit breakers and disconnectors [40], [41]. According to this standard, the preferential range of test levels includes: the 1st level is 0.5 kV, the 2nd level is 1 kV, the 3rd level is 2 kV and the 4th level is 4 kV. The oscillation frequencies are 0.1/1MHz for slow-damped oscillatory and 3/10/30 MHz for fast-damped oscillation. Compared with this standard, the measured peak values are between the 2nd and 3rd levels, the dominant frequencies are between 3 MHz and 30 MHz. As a result, the measured disturbance voltages can be covered by the 3rd level of the fast-damped oscillatory wave specified in the IEC 61000-4-18 standard.

2) ZERO-SEQUENCE VOLTAGE PORT AT THE SECONDARY SIDE OF THE TRANSFORMER

Figure 19 shows the voltage waveform of the zero-sequence voltage port on the secondary side of the transformer when the circuit breaker opens at 20 kA current. As shown in Fig. 19(b), the duration of the opening instant (t=0.099 s) pulse is about 187 μs, which is composed of three segments of micropulse. Each segment of micropulse lasts about 36 μs, and the peak value can reach 100 V. The spectrum of the micropulse with the largest peak value is shown in Fig. 20, and the dominant frequency is 5.74 MHz.

3) PHASE C CURRENT PORT AT THE SECONDARY SIDE OF THE TRANSFORMER

The current waveform of the phase C current port at the secondary side of the transformer is shown in Fig. 21. From the closing moment of the test station (t=0.00 s) to the opening moment of the prototype circuit breaker (t=0.07 s), the voltage waveform at the secondary side of the transformer is approximately a power frequency sine wave with a peak-to-peak value of 95 V. A pulse signal with a peak value of about 75 V appears at the moment of opening, and the duration is about 46 μs.

4) ZERO-SEQUENCE CURRENT PORT AT THE SECONDARY SIDE OF THE TRANSFORMER

The voltage waveform and corresponding frequency spectrum of the zero-sequence current port on the secondary side

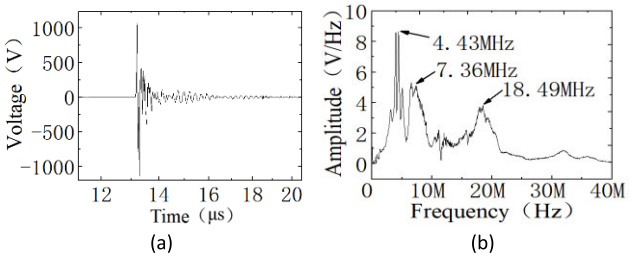

FIGURE 18. Electric quantity waveform at the primary side under opening conditions.

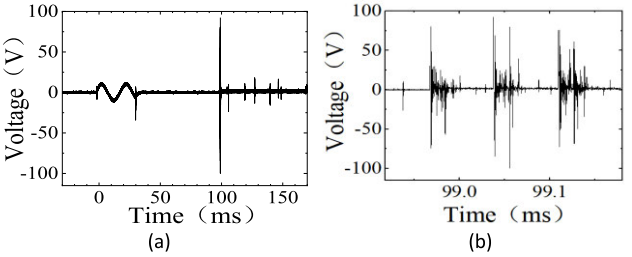

FIGURE 19. The voltage waveform of the zero-sequence voltage port at the secondary side of the transformer when the circuit breaker is opened: (a)overall waveform; (b)micropulse waveform at the moment of opening.

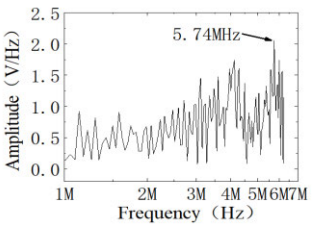

FIGURE 20. The spectrum of the maximum micro pulse at zero-sequence voltage port on the secondary side of the transformer when the circuit breaker is opened.

of the transformer are shown in Fig. 22. The peak value of the disturbance voltage is 185 V, the waveform duration is 68.5 ms, and it is composed of 12 micro pulse signals, with the dominant frequencies of 92 Hz and 288 Hz.

C. VOLTAGE BETWEEN ENCLOSURE AND GROUND

Take a measuring point on the switch enclosure as the measured point and take a wiring point on the grounding busbar on the wall about 2 meters away from the switch as the grounding point. The measured voltage waveform of the enclosure to the ground at the moment of closing and opening operation of the circuit breaker is shown in Fig. 23. Pulse signals appear at the moment of closing and opening, and the signal strength is higher when opening. The micropulse waveform is shown in Fig. 24. The pulse signal at the moment of closing lasts about 61 μs and consists of two micro pulses. The peak value of the first micropulse is 367 V, and the duration is 11.5 μs; The peak value of the second micropulse is 470 V, and the duration is 12 μs. The opening instantaneous pulse signal lasts about 299 μs and consists of 6 micro pulses. The minimum peak value of the micropulse is 204 V, the

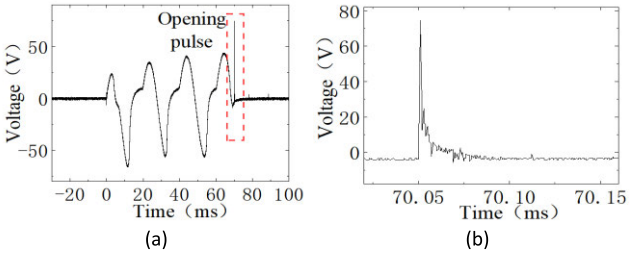

FIGURE 21. The waveform of the phase C current port at the secondary side of the transformer when the circuit breaker is opened: (a)overall waveform; (b)micropulse waveform at the moment of opening.

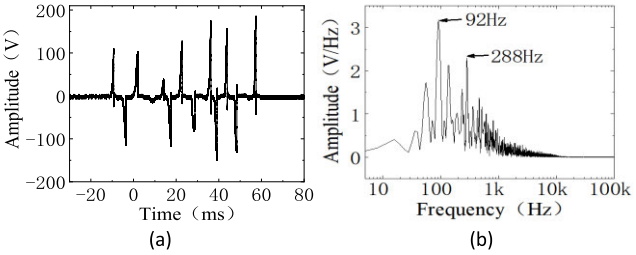

FIGURE 22. The waveform of the zero-sequence current port at the secondary side of the transformer when the circuit breaker is opened: (a)time domain waveform; (b) amplitude-frequency characteristic.

maximum value is 735 V and the average duration is about 40 μs.

D. FIELD INDUCED VOLTAGE

The 5-turn loop with a diameter of 15cm is placed one meter below the incoming line side of the circuit breaker. The loop and voltage probe are wrapped with aluminum foil to shield the electromagnetic disturbance of space field coupling. The magnetic field-induced voltage when the circuit breaker acts is shown in Fig. 25. At the moment of closing, the loop induces a fast-damped oscillatory wave with a peak value of about 40 V. After the signal is attenuated, a weak power frequency signal with a peak value of about 2 V can be observed. As shown in Fig. 26, the micropulse signal at the moment of closing has a total duration of about 391 μs and consists of four damped oscillatory waves. Each segment of the damped oscillatory wave has a duration of about 35 μs and a dominant frequency of about 732 kHz. The amplitude of the first two damped oscillatory is larger, and the peak value is 43 V; The latter two have smaller amplitudes, with a peak value of 23 V. It can be estimated approximately that the coupling voltage of the space magnetic field induced by a single turn loop with a diameter of 15 cm at this measuring point is about 8 V, while the physical size of the circuit board, in reality, is smaller, and the coupling voltage is also smaller. It can be considered that the space coupling is weak relative to the conductive coupling, so the impact of the space magnetic field on the electronic equipment can be ignored. In addition, the dominant frequency of the space magnetic field coupling voltage should be related to the physical size of the test site. The metal shielding enclosure of the test hall forms a huge cavity resonator, which causes high-frequency interference.

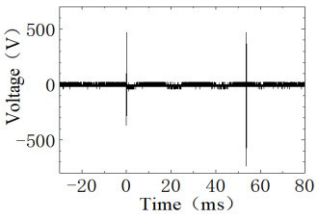

FIGURE 23. The voltage waveform of the enclosure to the ground when the circuit breaker is opened and closed.

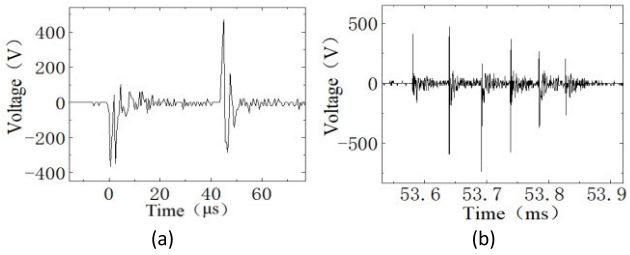

FIGURE 24. Micropulse waveform of the enclosure to ground voltage when the circuit breaker is opened and closed: (a) circuit breaker closing pulse signal; (b) circuit breaker opening pulse signal.

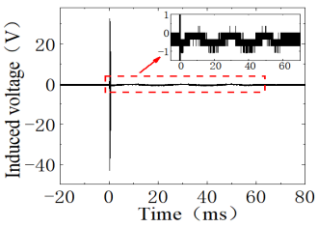

FIGURE 25. Loop-induced voltage.

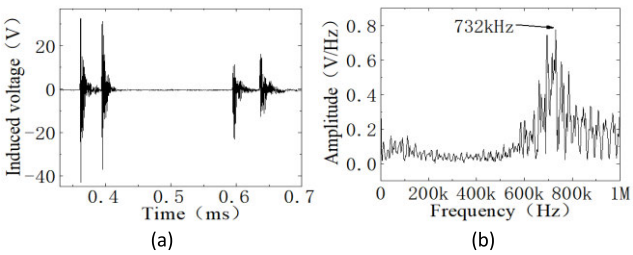

FIGURE 26. Loop-induced voltage when the circuit breaker is closed: (a) circuit breaker closing pulse signal; (b) amplitude-frequency characteristics of closing pulse.

When Ryszard et al. measured partial discharge and radio interference voltage in the high-voltage test hall, they also measured an oscillation signal with a frequency of about 1 MHz [38].

For damped oscillatory waves, 0.1 MHz and 1 MHz frequency points are generally used for assessment in the standard. Fig. 27 shows the standard waveforms in the damped oscillatory magnetic field immunity test, and Table 3 shows the preferred range of test levels [42]. While the measured waveform is not the standard damped oscillatory wave under these two frequency points, there is a standard equivalent conversion problem when assessing damped oscillatory

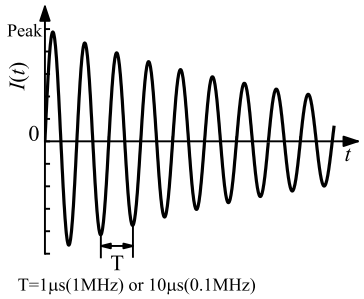

FIGURE 27. Standard damped oscillating magnetic field waveform.

TABLE 3. Test levels circuit breaker action measuring port disturbance voltage waveform parameters.

Level	Damped oscillatory magnetic field strength A/m (peak)
1	not applicable
2	not applicable
3	10
4	30
5	100
X[a]	special

NOTE The magnetic field strength is expressed in A/m; 1A/m corresponds to a free space magnetic flux density of 1.26 μT.
[a] "X" can be any level, above, below or in between the others. This level, as well the duration of the test, shall be specified in the dedicated equipment specification.

electromagnetic disturbance of other frequencies. Considering that the magnetic field affects the secondary equipment through the electromagnetic induction principle, that is, the induced voltage is generated on the circuit of the secondary equipment, so the peak value of the induced voltage can be used as a key indicator to evaluate the disturbance intensity. The induced voltage depends on dH/dt, so the peak value of dH/dt is selected to convert the assessment standard between damped oscillatory waves of different frequencies. Taking 0.1 MHz as an example, the rising edge time corresponding to this frequency is about 2.5 μs. Considering the highest level of immunity standard 100 A/m, the dH/dt peak value corresponding to 0.1 MHz is dH/dt $\approx$ (100 A/m) / (2.5 μs) $= 0.04\ \mathrm{kA{\cdot}m^{-1} \cdot \mu s^{-1}}$; Similarly, taking 1 MHz as an example, the peak value of dH/dt is $0.4\ \mathrm{kA{\cdot}m^{-1} \cdot \mu s^{-1}}$; The peak value of dH/dt corresponding to the measured disturbance waveform voltage peak value can be inferred as $0.387\ \mathrm{kA{\cdot}m^{-1} \cdot \mu s^{-1}}$. It can be seen from the comparison that dH/dt can only cover the peak dH/dt of the measured disturbance waveform when the frequency point is 1 MHz and the highest magnetic field strength is 100 A/m, that is, it needs to be assessed by the damped oscillatory magnetic field test grade 5 with a frequency of 1 MHz.

E. ELECTROMAGNETIC DISTURBANCE VOLTAGE PARAMETERS OF EACH MEASURING PORT

The power supply voltage of the circuit breaker on the primary and secondary integration column is 12 kV. The summary of the voltage waveform parameters of each test port when closing and opening 20 kA current is shown in Table 4. The waveform parameters listed are for the waveform

TABLE 4. The main characteristics of the waveforms of the electromagnetic disturbances for different operating cases and measured ports.

Signal port	Operation Type	Peak /V	Macro pulse duration /μs	Number of micro pulses	Micro-pulse duration /μs	Main frequency/MHz
A-phase voltage port	Closing and opening-closing	250	51.5	2	16.46 /7.14	4.43, 14.76
	Closing and opening-opening	250	185.66	6	45	4.11
C-phase voltage port	Closing and opening-closing	217	53.95	2	16.8/ 9.6	4.43, 6.11, 18.33
	Closing and opening-opening	220	280.1	6	45	4.41
	Closing	1100	6.04	1	/	4.43, 7.36, 18.49
Zero sequence voltage port	Closing and opening-closing	250	51.5	2	2	/
	Closing and opening-opening	250	286	6	3.5	/
	Closing	100	187	3	36	5.74
A-phase current port	Closing and opening-closing	266	51	2	3	/
	Closing and opening-opening	350	272	6	3.5	/
C-phase current port	Closing	75	46	1	46	/
Zero sequence current port	Closing and opening	160	52	10	/	92, 62, 202(Hz)
	Closing	185	68.5	12	/	92, 288(Hz)
enclosure - ground voltage	Closing and opening-closing	367	61	2	11.5	/
	Closing and opening-opening	735	299	6	40	/
Field-induced voltage	Closing and opening-closing	40	391	4	35	0.732

TABLE 5. Comparison the dH/dt of the damped oscillatory magnetic field specified in IEC 61000-4-10 standard and the measured result.

	Oscillation frequency	Level	dH/dt
IEC61000-4-10: *f*=0.1MHz	0.1 MHz	100A/m	$0.04\mathrm{kA{\cdot}m^{-1}{\cdot}\mu s^{-1}}$
IEC61000-4-10: *f*=1MHz	1 MHz	100A/m	$0.4\mathrm{kA{\cdot}m^{-1}{\cdot}\mu s^{-1}}$
Actually measured	0.732MHz		$0.387\mathrm{kA{\cdot}m^{-1}{\cdot}\mu s^{-1}}$

parameters of the tested port at the moment of opening and closing of the circuit breaker.

IV. CONCLUSION

The electromagnetic disturbances resulted from the switching operation of the primary and secondary integrated 10 kV circuit when the breaker 20 kA current was measured. The results show that the waveforms of disturbance voltages are damped oscillatory waves. The maximum disturbance voltage occurs at the phase voltage port with a peak value of 1.1 kV with the dominant frequencies of 4.4 MHz and 15 MHz. For other ports, the peak values are usually smaller than 500 V. The spatial magnetic field disturbance has a peak value of 0.387 kA/m/μs (dH/dt) and a dominant frequency of 0.732 MHz. According to these measured results, we conclude that the disturbance voltages can be covered by the third level (2.5 kV, 3 MHz, 10 MHz, and 30 MHz) of the fast-damped oscillatory wave defined in the immunity test method standard IEC 61000-4-18. Also, the magnetic fields can be covered by the fourth level (100 A/m, 0.1 MHz, and 1 MHz)of the damped oscillatory magnetic field defined in the immunity test method standard IEC 61000-4-10, as shown in Tab.5.

REFERENCES

[1] H.-T. Wu, C.-Q. Jiao, X. Cui, X.-F. Liu, and J.-F. Ji, "Transient electromagnetic disturbance induced on the ports of intelligent component of electronic instrument transformer due to switching operations in 500 kV GIS substations," *IEEE Access*, vol. 5, pp. 5104–5112, 2017.

[2] H. Wu, C. Jiao, X. Cui, X. Liu, and J. Ji, "Analysis and simulated experiment for port disturbance voltage due to switching operation in GIS substation," *High Voltage Eng.*, vol. 43, no. 10, pp. 3387–3395, 2017.

[3] X. Liu, X. Cui, H. Wu, J. Ji, and C. Jiao, "Measurement and analysis on electromagnetic disturbance of intelligent electronic device current transformer ports due to switching operations in a 500 kV gas insulated substation," *High Voltage Eng.*, vol. 41, no. 5, pp. 1709–1718, 2015.

[4] S. Ge, W. Liu, D. Ding, and X. Li, "Electromagnetic disturbance coupling and suppression of on-site electronic device power port in substations," *High Voltage Eng.*, vol. 47, no. 12, pp. 4483–4492, Dec. 2021.

[5] M. M. Rao, M. J. Thomas, and B. P. Singh, "Transients induced on control cables and secondary circuit of instrument transformers in a GIS during switching operations," *IEEE Trans. Power Del.*, vol. 22, no. 3, pp. 1505–1513, Jul. 2007.

[6] M. M. Rao, M. J. Thomas, and B. P. Singh, "Frequency characteristics of very fast transient currents in a 245-kV GIS," *IEEE Trans. Power Del.*, vol. 20, no. 4, pp. 2450–2457, Oct. 2005.

[7] D. Feng, M. Lu, J. Lan, and L. Sun, "Research on switching operation transient electromagnetic environment of substations in a coal mine," *IET Gener., Transmiss. Distrib.*, vol. 10, no. 13, pp. 3322–3329, Oct. 2016.

[8] Q. Wang, C. Fu, F. Chu, Y. Tong, X. Wang, G. Ye, and X. Wu, "A quantitative research on the level of disturbance to secondary signal ports of electronic voltage transformers under the operation of gas-insulated switchgear," *High Voltage*, vol. 7, no. 1, pp. 165–175, Feb. 2022.

[9] J. Zhao, W. Chen, and J. Zhang, "Analysis on electromagnetic compatibility immunity requirements for secondary equipment during switching transient operations in intelligent substation," *High Voltage Eng.*, vol. 41, no. 5, pp. 1686–1695, 2015.

[10] B. Liu, G. Ye, and Y. Tong, "Influence of disconnector in gas insulated switchgear switching on/off on electromagnetic compatibility of electronic transformer," *High Voltage Eng.*, vol. 44, no. 4, pp. 1204–1210, 2018.

[11] S. Bai, L. Zeng, M. Rong, Y. Li, K. Chen, and Y. Zhang, "Interference analysis and protection of electronic current transformer caused by disconnect switch operation in GIS," *High Voltage App.*, vol. 52, pp. 54–62, Jan. 2016.

[12] B. Liu, H. Huang, Y. Tong, and X. Deng, "Electromagnetic compatibility detection system of electronic transformer based on disconnector switching operation," *High Voltage Eng.*, vol. 44, no. 3, pp. 1016–1022, 2018.

[13] B. D. Russell, S. M. Harvey, and S. L. Nilsson, "Substation electromagnetic interference, Part I: Characterization and description of the transient EMI problem," *IEEE Power Eng. Rev.*, vol. PER-4, no. 7, p. 62, Jul. 1984.

[14] B. D. Russell, W. C. Kotheimer, and R. Malewski, "Substation electromagnetic interference, Part II: Susceptibility testing and EMI simulation in high voltage laboratories," *IEEE Power Eng. Rev.*, vol. PER-4, no. 7, p. 63, Jul. 1984.

[15] D. E. Thomas, C. M. Wiggins, F. S. Nickel, C.-D.-D. Ko, and S. E. Wright, "Prediction of electromagnetic field and current transients in power transmission and distribution systems," *IEEE Trans. Power Del.*, vol. 4, no. 1, pp. 744–755, Jan. 1989.

[16] D. E. Thomas, E. M. Wiggins, T. M. Salas, F. S. Nickle, and S. E. Wright, "Induced transients in substation cables: Measurements and models," *IEEE Trans. Power Del.*, vol. 9, no. 4, pp. 1861–1868, Oct. 1994.

[17] C. M. Wiggins, D. E. Thomas, F. S. Nickel, T. M. Salas, and S. E. Wright, "Transient electromagnetic interference in substations," *IEEE Trans. Power Del.*, vol. 9, no. 4, pp. 1869–1884, Oct. 1994.

[18] H. Wang, D. Huang, and X. Chen, "Research progress in electromagnetic disturbance characteristics and protection due to switching operations of primary and secondary integrated switchgear," *High Voltage Eng.*, vol. 48, no. 1, pp. 269–280, Jan. 2022.

[19] B. U. Musa, W. H. Siew, and M. D. Judd, "Computation of transient electromagnetic fields due to switching in high-voltage substations," *IEEE Trans. Power Del.*, vol. 25, no. 2, pp. 1154–1161, Apr. 2010.

[20] S. Ge, W. Liu, X. Li, and D. Ding, "Coupling characteristics of electromagnetic disturbance of on-site electronic device power port in substations and its suppression," *IEEE Trans. Electromagn. Compat.*, vol. 63, no. 5, pp. 1584–1592, Oct. 2021.

[21] G. Liu, P. Zhao, Y. Qin, M. Zhao, Z. Yang, and H. Chen, "Electromagnetic immunity performance of intelligent electronic equipment in smart substation's electromagnetic environment," *Energies*, vol. 13, no. 5, p. 1130, Mar. 2020.

[22] W. Chen, J. Zhao, K. Bian, D. Wang, B. Wan, Z. Zhou, J. Zhang, Z. Teng, X. Zhang, and Z. Li, "Research progress on transient electromagnetic disturbance due to switching operations in GIS substation," *Proc. CSEE*, vol. 39, no. 16, pp. 4935–4948, 2019.

[23] X. Chen, Z. He, Y. Zhang, J. Si, S. Wang, B. Wan, and J. Liu, "Research on conducted disturbance to secondary cable caused by disconnector switching operation," *Frontiers Energy Res.*, vol. 9, p. 898, Jan. 2022.

[24] A. Tatematsu, F. Rachidi, and M. Rubinstein, "Three-dimensional FDTD-based simulation of induced surges in secondary circuits owing to primary-circuit surges in substations," *IEEE Trans. Electromagn. Compat.*, vol. 63, no. 4, pp. 1078–1089, Aug. 2021.

[25] L. Cheng, Z. He, J. Liu, Z. Yang, X. Chen, Y. Zhang, S. Wang, and J. Si, "Research on radiated disturbance to secondary cable caused by disconnector switching operation," *Energies*, vol. 15, no. 5, p. 1849, Mar. 2022.

[26] L. Wang, J. Qian, J. Ji, Q. Bu, and Y. Yuan, "Modeling and characteristic analysis of switching transient disturbance in substation," *High Voltage Eng.*, vol. 43, no. 3, pp. 960–965, 2017.

[27] C. Li, W. Zhang, and J. Ji, "Disturbance voltage statistical characteristics of secondary system under impulse current and its consistency with immunity test," *Power Syst. Technol.*, vol. 45, no. 4, pp. 1605–1612, Apr. 2021.

[28] Y. Li, L. He, and C. Jiao, "Measurement and analysis of electromagnetic disturbance caused by switch operation of distribution switchgear," *Eng. Des.*, vol. 38, no. 11, pp. 57–63, Nov. 2019.

[29] P. Li, D. Huang, J. Ruan, X. Niu, Z. Pu, and C. Zhu, "The EMI study of pole-mounted switch's breaking on its secondary smart devices," *Trans. China Electrotechnical Soc.*, vol. 30, no. 8, pp. 27–37, 2015.

[30] B. Niu, J. Liu, and W. Shen, "Test and simulation of electromagnetic radiation interference during capacitive closing process of pole-mounted switch in distribution network," *High Voltage App.*, vol. 56, no. 377, pp. 11–16, 2020.

[31] W. Lu, J. Duan, L. Cheng, J. Lu, and X. Du, "Analysis of the influence of the breaking radiation magnetic field of a 10 kV intelligent circuit breaker on an electronic transformer," *Sensors*, vol. 21, no. 23, p. 7800, Nov. 2021.

[32] X. Chen, J. Zhu, and H. Zhao, "Study on electromagnetic interference of lightning shock to primary and secondary fusion set switches," *J. Zhengzhou Univ.*, vol. 41, no. 4, pp. 74–80, Jul. 2020.

[33] X. He, H. Zhao, and X. Cheng, "Influence of lightning impulse voltage on measurement accuracy of power distribution primary and secondary fusion equipment," *Electric Power Autom. Equip.*, vol. 40, no. 2, pp. 214–224, 2020.

[34] Q. Wang, Z. Teng, F. Chu, Y. Tong, J. Xiong, G. Ye, and X. Wu, "Experimental research on lightning disturbance characteristics of 10-kV fusion voltage transformer intelligent component acquisition port," *IEEE Access*, vol. 8, pp. 25905–25913, 2020.
[35] H. Wu, C. Jiao, and X. Cui, "Study on coupling of very fast transients to secondary cable via a test platform," *IEEE Trans. Electromagn. Compat.*, vol. 60, no. 5, pp. 1366–1375, Oct. 2018.
[36] H.-T. Wu, X. Cui, X.-F. Liu, C.-Q. Jiao, R. Hu, W.-J. Chen, and L. Wang, "Characteristics of electromagnetic disturbance for intelligent component due to switching operations via a 1100 kV AC GIS test circuit," *IEEE Trans. Power Del.*, vol. 32, no. 5, pp. 2228–2237, Oct. 2017.
[37] J. Zhang, C. Jiao, S. Li, M. Li, P. Zhao, and L. Lei, "Measurement and analysis of electromagnetic disturbance on the intelligent component CT port due to 500 kV gas insulated substation breaker operations," *High Voltage App.*, vol. 52, no. 8, pp. 29–36, 2016.
[38] R. Malewski, D. Train, and A. Dechamplain, "Cavity resonance effect in large HV laboratories equipped with electromagnetic shield," *IEEE Trans. Power App. Syst.*, vol. PAS-96, no. 6, pp. 1863–1871, Nov. 1977.
[39] *Testing and Measurement Techniques—Damped Oscillatory Wave Immunity Test*, Standard IEC 61000-4-18, 2019.
[40] *Electromagnetic Compatibility (EMC)—Part 6–5: Generic Standards-Immunity for Equipment Used in Power Station and Substation Environment*, Standard IEC 61000-6-5, 2015.
[41] *High-Voltage Switchgear and Controlgear—Part 1: Common Specifications for Alternating Current Switchgear and Controlgear*, Standard IEC 62271-1, 2017.
[42] *Testing and Measurement Techniques—Damped Oscillatory Magnetic Field Immunity Test*, Standard IEC 61000-4-10, 2016.

FEIYAN ZHOU was born in Hebei, China, in 1995. She received the B.E. and M.E. degrees in electrical engineering from Xi'an Jiaotong University, Xi'an, China, in 2017 and 2020, respectively. She is currently with the China Electric Power Research Institute. Her research interests include power distribution automation, fault detection, and EMC.

YAN WU was born in Nanyang, Henan, China, in 1982. She received the master's degree in electromagnetic field and microwave technology from North China Electric Power University, in 2010.

Since 2010, she has been engaged in the research of power distribution systems and equipment test technology with the Power Distribution Technology Center, China Electric Power Research Institute.

LINGYUN GU received the M.A.Eng. degree in materials science from North China Electric Power University, Beijing, China, in 2016. He is currently with the China Electric Power Research Institute. His research interests include the test and detection technology of distribution systems and medium and low-voltage complete sets of devices.

DINGYU QIN was born in Guangxi, China, in 1998. She received the B.Sc. degree in smart grid information engineering and the master's degree in electrical engineering from North China Electric Power University (NCEPU), Beijing, China, in 2020 and 2023, respectively. She is currently with the East China Branch of State Grid Corporation of China. Her research interests include electromagnetic shielding techniques and electromagnet compatibility in power systems.

CHONGQING JIAO was born in Hubei, China. He received the B.Sc. degree in geophysics from the Chinese University of Geosciences, Wuhan, China, in 2002, and the Ph.D. degree in physical electronics from the Institute of Electronics, Chinese Academy of Sciences, Beijing, China, in 2007. He is currently an Associate Professor of electrical and electronic engineering with North China Electric Power University, Beijing. His research interests include electromagnetic theory and applications and the EMC in power systems.

ZHANPENG DU was born in Tianjin, China, in 1997. He is currently pursuing the degree in electrical engineering with North China Electric Power University, Beijing, China. His research interests include spatial electromagnetic disturbance characteristics and suppression measures under the switching operation of substations.

ZUOXING DENG was born in Hunan, China. He received the B.Sc. degree in smart grid information engineering from North China Electric Power University (NCEPU), Beijing, China, in 2021, where he is currently pursuing the M.A.Eng. degree in electrical engineering. His research interests include the measurement and calculation of electromagnetic fields and the EMC in power systems.

ZHIYE JIANG was born in Hunan, China, in 1999. She received the B.E. degree in electrical engineering and automation from the Changsha University of Technology (CSUST), Hunan, in 2021. She is currently pursuing the M.A. Eng. degree in electrical engineering from North China Electric Power University, Beijing, China. Her research interests include electromagnetic shielding technology and electrode compatibility in power systems.

JIANCHENG HUANG was born in Inner Mongolia, China, in 1995. He is currently pursuing the degree in electrical engineering with North China Electric Power University, Beijing, China.

His research interest includes the simulation and distribution of electromagnetic fields in space.